

A Robertsonian translocation suppresses a somatic recombination pathway to loss of heterozygosity

Kevin M. Haigis & William F. Dove

Published online 25 November 2002; doi:10.1038/ng1055

In mammals, loss of APC/Apc gatekeeper function initiates intestinal tumorigenesis. Several different mechanisms have been shown or proposed to mediate functional loss of APC/Apc: mutation in *APC/Apc*, non-disjunction, homologous somatic recombination and epigenetic silencing. The demonstration that, in the C57BL/6 (B6) *Apc^{Min/+}* mouse model of inherited intestinal cancer, loss of Apc function can occur by loss of heterozygosity (LOH) through somatic recombination between homologs presents an opportunity to search for polymorphisms in the homologous somatic recombination pathway. We report that the Robertsonian translocation *Rb(7.18)9Lub (Rb9)* suppresses the multiplicity of intestinal adenomas in this mouse model. As the copy number of *Rb9* increases, the association with the interphase nucleolus of the rDNA repeats centromeric to the *Apc* locus on Chromosome 18 is increasingly disrupted. Our analysis shows that homologous somatic recombination is the principal pathway for LOH in adenomas in B6 *Apc^{Min/+}* mice. These studies provide additional evidence that neoplastic growth can initiate in the complete absence of canonical genomic instability.

Introduction

Familial adenomatous polyposis (FAP), or Gardner syndrome (OMIM 175100), is an autosomal dominant disease caused by a germline mutation in the adenomatous polyposis coli (*APC*) tumor-suppressor gene¹. Individuals with FAP can develop several thousand benign polyps throughout the colon. FAP belongs to a group of familial conditions known as the phakomatoses, in which a large number of benign lesions develop randomly throughout the affected tissue². The phenotypes of the phakomatoses are consistent with a model in which lesions are initiated by the stochastic inactivation of a tumor-suppressor gene.

Mouse models of human cancer syndromes have become powerful tools for analyzing disease pathogenesis. The phenotype of *Apc^{Min/+}* mice closely resembles that of humans with FAP; they develop multiple intestinal neoplasms³. *Apc^{Min/+}* mice are heterozygous with respect to a nonsense allele of *Apc*. This mouse model holds a great advantage over other experimental models of intestinal neoplasia, such as xenografts in nude mice, because the tumors are autochthonous and the neoplastic pathway shares with most human colonic tumors the loss of *APC/Apc* function. Thus, the *Apc^{Min/+}* mouse allows for the study of many aspects of tumor biology in the natural genetic and developmental environment.

Loss of function of the wild-type allele of *Apc* is necessary for tumorigenesis in *Apc^{Min/+}* mice, regardless of genetic background^{4,5}. On the B6 genetic background, loss of *Apc* function occurs exclusively by loss of heterozygosity (LOH)⁴, due, at least in part, to somatic recombination between homologs⁶.

The standard laboratory mouse karyotype consists of 40 acrocentric chromosomes, 19 pairs of autosomes and one pair of sex chromosomes. But wild races of *Mus musculus* often have karyotypes with centric fusions between acrocentric chromosomes to generate metacentrics, referred to as Robertsonian (Rb) translocations⁷. *Rb(7.18)9Lub* (hereafter referred to as *Rb9*), originally identified in a wild mouse caught in the Orobian Alps near Bergamo in Northern Italy⁸, consists of a centric fusion between Chromosomes 7 and 18. In addition to reduced fertility owing to meiotic non-disjunction, the chromosomes involved in a Robertsonian translocation show suppressed meiotic recombination when heterozygous^{9,10}. The suppression of recombination is thought to result from mispairing of trivalents during pachytene^{11,12}.

Recently, we have used the Robertsonian translocation, *Rb9*, to analyze the mechanism of LOH in tumors from B6 *Apc^{Min/+}* mice⁶. Here we delve more deeply into the somatic consequences of heterozygosity and homozygosity with respect to this Robertsonian translocation. Our central goal was to determine whether *Rb9* could suppress homologous somatic recombination, thereby suppressing tumor multiplicity in *Apc^{Min/+}* mice. Indeed, we found that *Rb9* is a potent suppressor of tumor multiplicity in B6 *Apc^{Min/+}* mice. We tested a series of hypotheses to explain the *Rb9* effect on intestinal tumorigenesis. These studies implicate *Rb9* in the direct, physical suppression of somatic recombination through mislocalization of the homologous Chromosome 18 centromeric regions in relation to each other and to the nucleolus. Our studies also tested

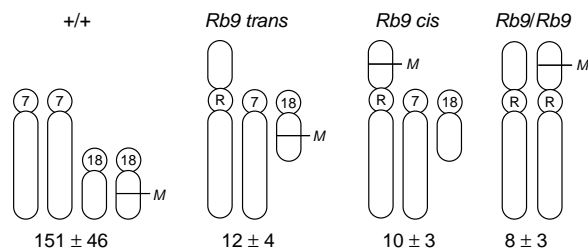


Fig. 1 *Rb9* acts as a suppressor of tumor multiplicity in *Apc*^{Min/+} mice. For each genotypic class, the complement of involved chromosomes is depicted. The average tumor multiplicity for each class is shown below the chromosome complement. R denotes the *Rb9* chromosome and M the *Min* allele of *Apc*. The numbers of mice generated for each class were as follows: karyotypically normal (+/+) = 16, *Rb9 trans* = 17, *Rb9 cis* = 15 and *Rb9/Rb9* = 18. Whereas data from a Poisson distribution would have a coefficient of dispersion (c.d. = variance/mean) of 1, the c.d. for the karyotypically normal mice presented here was 14, indicating that these tumors did not develop at random. In contrast to the karyotypically normal mice, tumor multiplicities from *Rb9*^{+/+} and *Rb9/Rb9* *Apc*^{Min/+} mice approached a Poisson distribution, as the variance (s.d.²) was nearly equal to the mean. The c.d. values for *Rb9 trans*, *Rb9 cis* and *Rb9/Rb9* were 1.3, 0.9 and 1.1, respectively. A global analysis of variation indicated that tumor multiplicities in *Rb9 trans* and *Rb9 cis* mice followed a Poisson distribution (see Web Note A online).

whether the principal (or sole) LOH pathway for early adenoma formation in the *Min* mouse involves homologous somatic recombination rather than karyotypic instability.

Results

***Rb9* is a semi-dominant suppressor of tumor multiplicity**

To determine whether *Rb9* can modify the tumor phenotype of *Apc*^{Min/+} mice, we generated mice that carry one or two copies of the translocation chromosome. Mice heterozygous with respect to *Rb9* (*Rb9*^{+/+}) carried the *Min* allele either on the wild-type acrocentric homolog (*Rb9 trans*) or else on the metacentric translocation chromosome (*Rb9 cis*). *Rb9 trans Apc*^{Min/+} mice developed markedly fewer intestinal adenomas at 60 days of age than did their littermates without the translocation (12 ± 4 and 151 ± 46, respectively; Fig. 1). *Rb9 cis* and homozygous *Rb9/Rb9* mice also developed fewer adenomas (10 ± 3 and 8 ± 3, respectively) at 60 days of age than did those not carrying *Rb9* (Fig. 1).

We used the Tukey–Kramer test, which evaluates multiple simultaneous comparisons between classes with different sample sizes¹³, to determine if the differences in tumor multiplicities between different *Rb9* classes were statistically significant. The *Rb9/Rb9* genotypic class differed significantly from the *Rb9 trans* class (*P* < 0.05), but not from the *Rb9 cis* class (*P* > 0.05; Table 1). Comparing the two heterozygous classes jointly against the *Rb9* homozygous class by Wilcoxon Rank Sum analysis, however, indicated that the *Rb9/Rb9* class differed significantly from the combined *Rb9* heterozygous class (*P* = 0.002). These analyses indicated that *Rb9* is a semi-dominant suppressor of tumor multiplicity.

Table 1 • Tukey–Kramer test of significance between *Rb9* tumor multiplicities^a

	<i>Rb9 trans</i>	<i>Rb9 cis</i>	<i>Rb9/Rb9</i>
<i>Rb9 trans</i>		2.88	2.75
<i>Rb9 cis</i>	1.58		2.85 ^b
<i>Rb9/Rb9</i>	3.93 ^b	2.38	

^aArithmetical differences between the means of the two classes are entered below the diagonal line; minimum significant difference (m.s.d.) values are given above the diagonal line. ^bTwo classes are significantly different at *P* = 0.05 when the difference between the means exceeds the m.s.d.

Statistical interdependence of tumor formation in *Min* mice

In pursuing the effects of Robertsonian fusions on tumor multiplicity, we made a notable statistical observation. Tumor multiplicities from B6 *Apc*^{Min/+} mice manifested as a clumped Poisson distribution, a phenomenon common to quantitative data from experimental mice¹⁴. By contrast, tumor multiplicities of *Apc*^{Min/+} mice carrying the *Rb9* karyotypic suppressor fit a Poisson distribution (Fig. 1; see Web Note A from M. A. Newton online).

***Rb9* affects tumor initiation, not growth rate**

A modifier of adenoma multiplicity in *Apc*^{Min/+} mice could act by controlling tumor initiation (for example, *Mlh1*) and/or by affecting the net growth rate of the adenoma (for example, *Mom1* (*Pla2g2a*) and *Dnmt1*; refs. 15–17). A specific mechanism by which the *Rb9* translocation might affect the growth rate of *Min*-induced adenomas involves the deletion of rDNA repeats on proximal Chromosome 18 by the centric fusion. This deficiency of rDNA might selectively compromise protein synthesis in the adenoma and thereby negatively impact tumor growth rate. Fluorescence *in situ* hybridization (FISH) to the *Rb9* chromosome with a probe specific to 28S rDNA repeats showed that at least a portion of the repeats was retained (data not shown). We investigated the hypothesis of growth rate deficiency by comparing the distributions of adenoma sizes at 60 days in *Apc*^{Min/+} mice with a normal karyotype to those with an *Rb9 trans* karyotype (Fig. 2a). These distributions were not significantly different by the Wilcoxon Rank Sum test (*P* = 0.41) and gave average maximum diameters of 0.90 ± 0.41 mm for the normal karyotype and 0.83 ± 0.38 mm for the *Rb9 trans* karyotype.

A number of genetic and environmental factors affect the regionality of adenomagenesis in the *Min* mouse (K.M.H., work in progress). Therefore, we investigated whether the effect of the *Rb9* translocation on tumor multiplicity involved the regional distribution of tumors over the intestinal tract. Tumors developed preferentially in the distal region of the small intestine in *Apc*^{Min/+} and *Apc*^{Min/+} *Rb9 trans* mice (Fig. 2b). We characterized regionality by assigning tumors to 2-cm segments from the stomach to the ileocecal junction, and established by the Wilcoxon Rank Sum test that there was no statistically significant difference in regionality between karyotypically normal *Apc*^{Min/+} and *Apc*^{Min/+} *Rb9 trans* mice (*P* = 0.47). Taken together, these results implicate *Rb9* as a suppressor of tumor initiation.

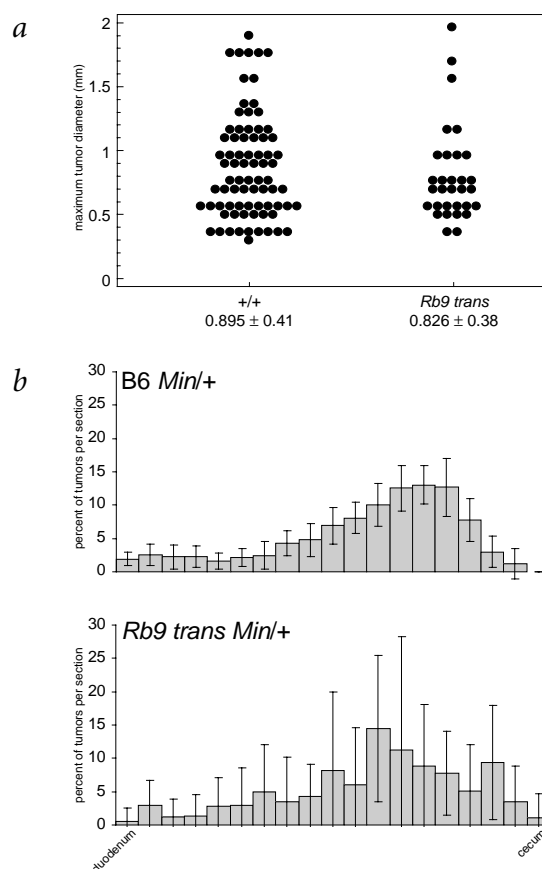
***Rb9* is a suppressor of somatic recombination**

The mechanism of LOH for tumors in B6 *Apc*^{Min/+} *Rb9/Rb9* mice includes somatic recombination⁶. Two mechanisms of LOH may exist in karyotypically normal B6 *Apc*^{Min/+} mice: somatic recombination and the production of cells carrying two copies of the mutated homolog (chromosomal homozygosis). The latter involves nondisjunction. Introduction of *Rb9* would interfere with the non-disjunction pathway, but leave the somatic recombination pathway intact. This model could explain the suppressive effect of *Rb9* on tumor multiplicity.

We evaluated the non-disjunction model (Fig. 3). LOH by chromosomal homozygosis predicts an unbalanced karyotype in tumors from *Apc*^{Min/+} *Rb9*^{+/+} mice. Selection against an unbalanced karyotype in the adenoma would account for the suppression of tumor multiplicity in *Apc*^{Min/+} *Rb9*^{+/+} mice. But this scenario does



Fig. 2 *Rb9* does not affect tumor size or regional distribution. **a**, Each dot represents the maximum diameter of a single tumor from karyotypically normal (+/+) or *Rb9 trans* mice. The average maximum tumor diameter (\pm s.d.) is given below the genotype. There was no significant difference in tumor size distributions between the two classes ($P = 0.41$, Wilcoxon Rank Sum test). **b**, Each vertical bar represents the average percentage of total tumors that developed in the indicated 2-cm sections of the small intestine. For the karyotypically normal (+/+) class, all of the tumors from each of 20 mice were counted; for *Rb9 trans*, all of the tumors from each of 12 mice were counted. There was no significant difference between the two distributions ($P = 0.47$).



not explain why tumor multiplicity is suppressed in *Apc^{Min/+} Rb9/Rb9* mice, where diploid tumors resulting from non-disjunction would have a balanced karyotype. In evaluating the importance of the postulated non-disjunction pathway, one must also consider the karyotypic imbalances for the predicted intermediate stages en route to homozygosis of the chromosome carrying the *Min* allele. Homozygosis could follow either a monosomic or trisomic intermediate, depending on when the chromosome carrying the *Apc⁺* allele is lost. In the former case, the phenotype of karyotypically normal mice would be equivalent to that of *Rb9 cis* mice, and the phenotype of *Rb9 trans* mice would be equivalent to that of *Rb9/Rb9* mice (Fig. 3a). In the latter case, the phenotype of karyotypically normal mice would be equivalent to that of *Rb9 trans* mice, and *Rb9 cis* would be phenotypically equivalent to *Rb9/Rb9* (Fig. 3b). None of these predicted phenotypic equalities was borne out under experimental scrutiny. Instead, *Rb9 trans* was equivalent to *Rb9 cis* ($P = 0.1$), and each was significantly different from karyotypically normal mice ($P = 0.002$). Thus, the non-disjunction pathway does not explain the semi-dominant nature of tumor suppression in *Apc^{Min/+}* mice carrying *Rb9* translocations. This analysis indicates that the suppression of tumor multiplicity by *Rb9* cannot

be explained by the existence of a principal non-disjunctional LOH pathway that is selectively eliminated in translocation-bearing mice.

Under conditions in which the LOH pathway of tumorigenesis has been strongly suppressed, as when the *Min* allele is congenic on the AKR/J background, a class of adenomas is found in which the *Apc* locus remains heterozygous (*Apc^{Min/+}*) and the wild-type *Apc* allele is seemingly silenced rather than lost or mutated⁶. The mechanism by which these ‘maintenance of heterozygosity’ (MOH) adenomas arise is not yet understood. We assayed LOH in the tumors arising in *Apc^{Min/+}* mice carrying *Rb9* translocations by assessing the ratio of *Apc⁺* to *Apc^{Min}* alleles by quantitative PCR (Table 2). On the karyotypically normal background, 24 of 25 tumors that we scored showed LOH, which is consistent with previous findings⁴. In *Rb9/+ trans* mice, the frequency of LOH tumors fell to 22 of 30 (73%), and in *Rb9/Rb9* mice the frequency fell further to 24 of 40 (60%). An overall accounting (Table 2) indicated that each copy of the *Rb9* translocation affected only the LOH class of adenoma. Thus, the

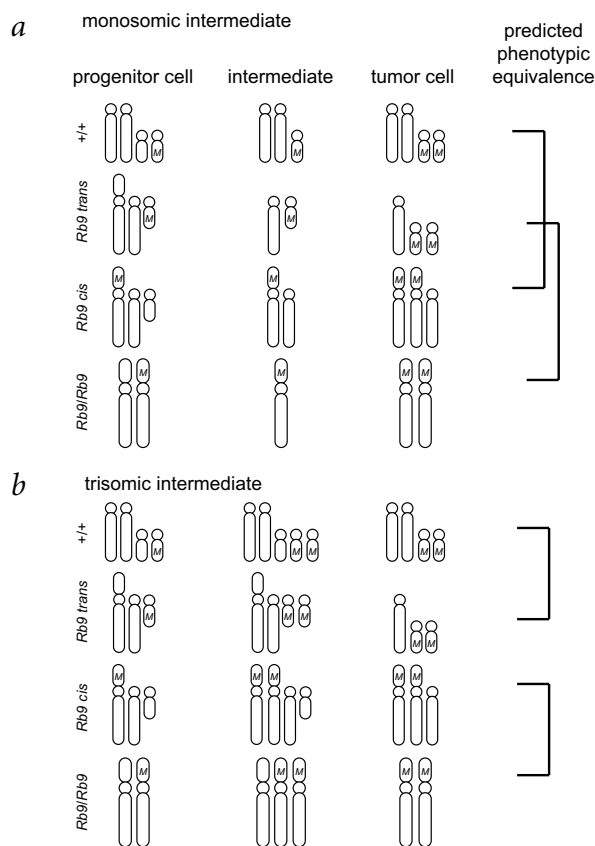


Fig. 3 Formal evaluation of the hypothesis of a principal non-disjunctional LOH pathway. **a**, If homozygosity with respect to the chromosome carrying the *Min* allele (*M*) proceeded through a monosomic intermediate, the phenotype of karyotypically normal (+/+) mice would be equivalent to that of *Rb9 cis* mice, because both postulated intermediates are monosomic for Chromosome 18 and disomic for Chromosome 7. *Rb9 trans* mice would have the same phenotype as *Rb9* homozygous mice because the postulated intermediates are monosomic for both Chromosomes 7 and 18. **b**, If the chromosome carrying the *Min* allele became homozygous through a trisomic intermediate, then the karyotypically normal (+/+) phenotype would be equivalent to the *Rb9 trans* phenotype because each of these postulated intermediates is trisomic for Chromosome 18 and disomic for Chromosome 7. *Rb9 cis* and *Rb9/Rb9* would be equivalent, because each postulated intermediate is trisomic for both Chromosomes 7 and 18. None of these predictions fits our experimental observations, indicating that suppression by *Rb9* does not involve extinction of a principal non-disjunctional LOH pathway.

Table 2 • LOH analysis of *Rb9* *Apc*^{Min/+} tumors

Genotype	Tumor multiplicity, mean ± s.d.	Class	Number	Tumor multiplicity by class	<i>Apc</i> ^{+/+} / <i>Apc</i> ^{Min} ratio, mean ± s.d.
Karyotypically normal	151 ± 46	LOH tumors	24/25 (96%)	144	0.161 ± 0.055
		MOH tumors	1/25 (4%)	6	0.603
		Normal controls	9		0.743 ± 0.085
<i>Rb9</i> trans	12 ± 4	LOH tumors	22/30 (73%)	9	0.141 ± 0.060
		MOH tumors	8/30 (27%)	3	0.676 ± 0.19
		Normal controls	11		0.727 ± 0.25
<i>Rb9/Rb9</i>	8 ± 3	LOH tumors	24/40 (60%)	5	0.216 ± 0.097
		MOH tumors	16/40 (40%)	3	0.780 ± 0.22
		Normal controls	8		0.753 ± 0.12

translocation selectively affected the production of somatic recombinants. We have noted above and in Web Note A that the distribution of tumor multiplicities in mice heterozygous for *Rb9* is random (Poisson), in contrast with the non-random (clumped Poisson) distribution observed in karyotypically normal *Apc*^{Min/+} mice in which LOH predominates over the MOH pathway. The non-random character of the LOH pathway may mirror the fact that most adenomas in B6 *Apc*^{Min/+} mice, and in one individual with FAP, are polyclonal in structure^{18,19}.

One hypothesis for the suppression of recombination in *Rb9* cells is that the wild-derived *Rb9* chromosome carries sequence polymorphisms compared with the B6 Chromosome 18 (ref. 20). To test this hypothesis, we screened for microsatellite polymorphisms between B6 and its *Rb9* derivative throughout Chromosome 18. We found no polymorphic microsatellites from *D18Mit19* (2 cM) to *D18Mit213* (55 cM), indicating that most, if not all, of Chromosome 18 was derived from B6. We cannot rule out the existence of sequence polymorphisms proximal to *D18Mit19*, the region most important for the recombinational LOH event. But, crucially, *Rb9* suppressed LOH more strongly in homozygous form than when heterozygous. This rules out the hypothesis that sequence heterozygosity is responsible for the suppression of recombination.

Mislocalization of the *Rb9* chromosome

In tumors from B6AKRF1 *Apc*^{Min/+} mice, LOH occurs along the entire Chromosome 18, indicating that somatic recombination occurs preferentially in the proximal region of this chromosome⁴. One level at which interference of recombination by *Rb9* could occur is in the interphase localization to the nucleolus of the centromeric nucleolar organizing regions (NOR) of Chromosome 18. We analyzed the association of the NOR with the nucleolus through a combination of FISH and immunohistochemistry. In fibroblasts containing two acrocentric copies of Chromosome 18, a FISH probe for the Chromosome 18 centromere (*18cen*) always was found within 1 μm of the periphery of the nucleolus (Fig. 4a). By contrast, a probe for the Chromosome 14 centromere (*14cen*), a chromosome without an rDNA repeat, was rarely found within 1 μm of the nucleolar periphery and commonly was localized more than 3 μm away (Fig. 4d). In *Rb9/+* and *Rb9/Rb9* cells, the *18cen* signals also localized near the nucleolus, indicating that the *Rb9* chromosome could integrate into the nucleolus (Fig. 4b,c). One qualitative difference between karyotypically normal (+/+) and *Rb9* cells concerned the positioning of the two *18cen* signals with respect to the nucleolus. In karyotypically normal cells, the two *18cen* signals tended to lie near each other, on the same side of the nucleolus. By contrast, the *18cen* signals in *Rb9/+* and *Rb9/Rb9* cells often localized to opposite sides of the nucleolus (Fig. 4b), indicating that, at least in fibroblasts, the *Rb9* chromosome was not integrated into the nucleolus in the same way as was the acrocentric Chromosome 18.

To determine whether the Chromosome 18 homologs were mislocalized relative to each other in the intestinal epithelium itself, we analyzed the distances between the Chromosome 18 centromeres in cells from this tissue. To do so, we carried out interphase FISH on 5-μm tissue sections from intestines of karyotypically normal, *Rb9/+* and *Rb9/Rb9* mice. We determined the projected planar distance between hybridization signals with the probes *18cen*, *18tel*

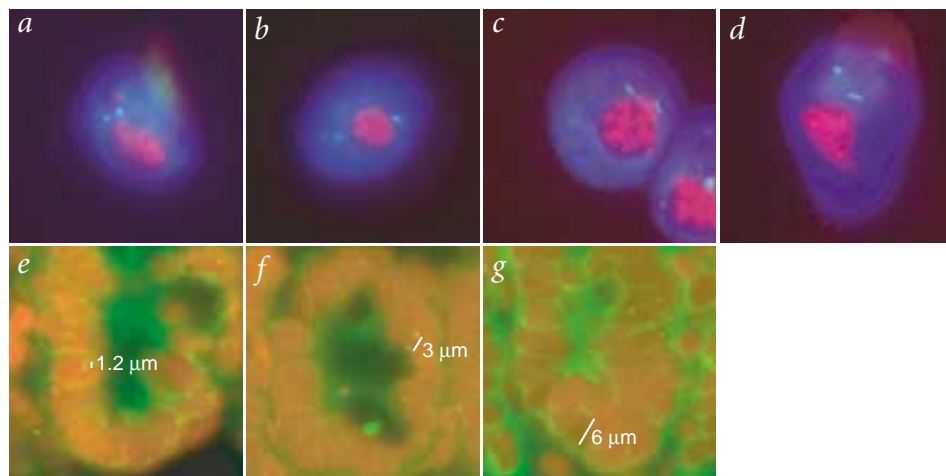


Fig. 4 Nuclear localization of centromeres. **a–d**, Interphase FISH and immunohistochemistry were carried out on primary fibroblasts carrying zero, one or two copies of *Rb9*. **a**, In karyotypically normal (+/+) cells, the *18cen* signals (green) were found near the nucleolus (red) and typically near each other. **b**, In *Rb9/+* cells, the *18cen* signals were also found near the nucleolus but were frequently contralateral. **c**, In *Rb9/Rb9* cells, the *18cen* signals were localized near the nucleolus. **d**, As a control, a probe specific to the centromere of Chromosome 14, which does not have an NOR, was used. The *14cen* signals were usually located far from the nucleolus. Sometimes, by chance, one, but not both, of the signals was found near the periphery of the nucleolus. For each genotype, at least 10 cells were examined for localization of the centromeric signals. **e–g**, Measurement of the two-dimensional projection of the distance between Chromosome 18 signals with interphase FISH. This figure shows extreme examples representative of each class, with the distance between the two signals indicated. **e**, karyotypically normal (+/+); **f**, *Rb9/+*; **g**, *Rb9/Rb9*.



and an interstitial probe (*Apc*) (Table 3 and Fig. 4e–g). The consistent inter-homolog distance in karyotypically normal cells provided evidence for co-localization of the homologous segments in interphase nuclei. In karyotypically normal cells, the *18cen* and *18tel* signals were separated in two-dimensional space by an average of roughly 2.0 μm and roughly 2.3 μm , respectively, whereas the *Apc* signals lay roughly 2.9 μm apart (Table 3). In *Rb9/+* and *Rb9/Rb9* cells, the spacings of homologous *Apc* and *18tel* signals were the same as in karyotypically normal cells. By contrast, in these cells, the homologous centromeric segments were more widely separated than in karyotypically normal cells, by 3.0 μm in *Rb9/+* and 4.5 μm in *Rb9/Rb9*, compared with 2.0 μm in cells from karyotypically normal mice (Table 3). The distributions of projected distances were significantly different between the genotypic classes. Thus, the *Rb9* centromere seemed to home to the nucleolus but mislocalized in the detailed nucleolar assembly. These results support the hypothesis that *Rb9* affects the pairing of the homologous substrates controlling the somatic recombination event.

Discussion

Translocations generate novel joints of DNA sequence that can provoke tumorigenesis through activation of proto-oncogenes or loss of tumor-suppressor gene function. By contrast, the novel joints involved in Robertsonian translocations have been thought to be phenotypically benign in the soma. We found, however, that a Robertsonian translocation can exert a profound somatic phenotype: mice carrying one or two copies of the Robertsonian translocation *Rb9* have markedly lower intestinal tumor multiplicity. We provided evidence against suppression of tumor growth rate or of non-disjunction as the mechanism by which *Rb9* reduces tumor multiplicity. Further, with the exception of the possible deletion of *rDNA* repeats involved in the centric fusion, the translocation strains were isogenic to B6, so that no other modifier locus could be involved in the suppression that we observed. Instead, our results indicate that *Rb9* suppresses homologous somatic recombination on Chromosome 18. Thus, *Rb9* exemplifies a modifier of tumorigenesis involving polymorphic karyotypic organization rather than sequence heterozygosity or polymorphic gene activity.

Which stage in recombinant production is impaired by the translocation? One hypothesis is that the *Rb9* effect on somatic recombination occurs early during recombination; for example, at the stage of pairing of the homologous substrates. An alternate hypothesis is that *Rb9* affects the production of recombinants at a later stage. *Rb9* could affect the resolution of the recombinant chromatids, or daughter cells containing certain recombinant genotypes could have a selective disadvantage. Our data are consistent with an effect on substrate pairing.

We observed that the *Rb9* chromosomes were mislocalized near the centromere but not near the telomere. This observation is notable given the distribution of LOH along Chromosome 18 in tumors from *Apc^{Min/+}* mice. It has previously been shown that each LOH event affects the entire length of Chromosome 18 in tumors from B6AKRF1 *Apc^{Min/+}* mice⁴. To understand how *Rb9* could suppress somatic recombination, we sought to understand the molecular identity of this postulated recombination hot spot.

Table 3 • Two-dimensional spacing between Chromosome 18 homologs in intestinal epithelial cells

Cell genotype	Inter-homolog spacing (μm), mean \pm s.d. (n)		
	<i>18cen</i> ^a	<i>Apc</i> ^b	<i>18tel</i> ^b
+/+	1.97 \pm 1.0 (39)	2.86 \pm 1.3 (69)	2.33 \pm 1.1 (52)
<i>Rb9/+</i>	3.03 \pm .99 (28)	2.83 \pm 1.4 (37)	2.20 \pm 1.3 (41)
<i>Rb9/Rb9</i>	4.53 \pm 1.6 (24)	3.31 \pm 1.8 (48)	2.06 \pm .97 (24)

^aThe distributions of two-dimensional distances in this column were significantly different by Wilcoxon Rank Sum analysis. The *P* values were as follows: karyotypically normal (+/+) versus *Rb9/+*, *P* = 5.6 \times 10⁻⁶; karyotypically normal (+/+) versus *Rb9/Rb9*, *P* = 4.0 \times 10⁻⁸; *Rb9/+* versus *Rb9/Rb9*, *P* = 3.8 \times 10⁻⁴. ^bNone of the pairwise comparisons in this column were statistically different (*P* > 0.2, Wilcoxon Rank Sum test).

A good candidate for the hot spot is *Rnr18*, the *rDNA* repeat that lies near the centromere of Chromosome 18. NORs, which are composed of *rDNA* repeats, are known to be common sites of recombination in somatic cells. An appealing hypothesis is that somatic recombination occurs at double-strand breaks arising at replication forks stalled within *rDNA* repeats. Studies in *Escherichia coli* indicate that arrest at replication forks is recombinogenic²¹. Indeed, in all organisms studied, homologous recombination serves to repair stalled replication forks²².

What factors control recombination in the soma? Mutations in such genes as the Bloom syndrome helicase (*Blm*), poly(ADP-ribose) polymerase (*Adprt1*) and *Trp53* have been directly shown to increase the frequency of somatic recombination *in vivo*^{23–25}. Mutation of *Blm* also increases tumor multiplicity in *Apc^{Min/+}* mice through stimulation of inter-homolog recombination on Chromosome 18 (ref. 23). In contrast with proteins that normally suppress somatic recombination, proteins including Rad54, Brca1, Brca2 and *Xrcc4* promote homologous somatic recombination²⁶. Notably, cells from mice carrying a mutation in the gene associated with ataxia–telangiectasia (*Atm*) do not have increased recombinational LOH compared with cells from wild-type mice²⁷.

Sequence divergence has also been shown to suppress homologous somatic recombination. It has been shown that LOH at the *Aprt* locus is suppressed in cells from hybrids between distantly related mouse strains²⁰. This suppression of recombination involves the DNA mismatch repair pathway; loss of mismatch repair function leads to an increase in recombination between divergent sequences but does not affect recombination between identical sequences²⁸. Recombinant production is suppressed in the soma of experimental mice carrying other chromosomal abnormalities such as inversions or reciprocal translocations^{29,30}. Suppression by *Rb9* is unique, however, in that it is stronger when *Rb9* is homozygous. These other karyotypic abnormalities, by contrast, probably suppress recombination only when heterozygous³¹.

Finding that the *Rb9* translocation suppresses somatic recombination even when homozygous establishes that it affects an early stage of the recombination process. Our studies have identified a third component of the system regulating somatic recombination, the intranuclear localization of homologous recombination substrates. We can now formulate a more complete model of recombination between homologs in somatic cells. To recombine at relatively high frequency, the homologous segments must (i) co-localize and pair, at least transiently, during interphase; (ii) share highly similar, if not identical, sequence; and (iii) assemble the proper molecular machinery.

The development of human colorectal cancer has been proposed to require a mutator phenotype in the form of either microsatellite or karyotypic instability³². Is genomic instability necessary for cancer initiation³³? We have shown recently that LOH in adenomas from *Apc^{Min/+}* mice can occur by somatic recombination, and that adenomas from mice and humans have





stable microsatellites and a stable karyotype⁶. Here we provide evidence that the tumor-initiating LOH event in Min mice occurs largely, if not exclusively, by somatic recombination. Thus, it seems that neoplastic growth can initiate in the complete absence of either canonical form of genomic instability.

Robertsonian translocations are the most common structural abnormality of human chromosomes, occurring at a frequency of 1 in 1,000 births³⁴. In humans, Robertsonian translocations develop between the acrocentric chromosomes that carry the NORs at their centromeric ends, namely, Chromosomes 13, 14, 15, 21 and 22. Carriers of these translocations are identified clinically by a generalized reduction in fertility, a phenotype common to Robertsonian-translocation heterozygotes³⁵.

Is the suppression of homologous somatic recombination by Robertsonian translocations a factor in human cancer? It has been shown that NOR function is commonly lost in human Robertsonian chromosomes involving deletion of rDNA repeats during the formation of the translocation³⁶. The most common Robertsonian translocation in humans is *Rb(13q.14q)*, which accounts for 70% of all centric fusions. On human Chromosome 13 resides the prototypic tumor suppressor, the retinoblastoma gene (*RB*). At least one third of the cases of LOH in retinoblastoma involve somatic recombination³⁷. Thus, the presence of a Robertsonian translocation could be responsible for the non-penetrant cases of retinoblastoma not explained by weak *RB* alleles³⁸. By contrast, *APC* is located on Chromosome 5, which is not known to be involved in Robertsonian translocation.

It will be interesting to determine whether inversions and reciprocal translocations, which occur at frequencies similar to Robertsonian translocations in humans³⁹, also show karyotypic suppression of somatic recombination, and in doing so protect against LOH and cancer. We note that the frequency of chromosome abnormalities in human populations is probably increasing owing to assisted fertility by *in vitro* fertilization and intracytoplasmic sperm injection³⁵. Aside from their involvement in Robertsonian translocations, rDNA repeats themselves can also be polymorphic in length and thereby contribute to variable probability of somatic recombination.

We have shown for the first time that certain chromosomal configurations can protect against cancer: a rearrangement by centric chromosome fusion can act as a polymorphic genetic modifier of tumorigenesis. We show that loss of heterozygosity owing to somatic recombination is less frequent when the two homologous substrates are mislocalized with respect to each other in the nucleus. These studies implicate chromosomal segment localization within the nucleus as an important factor in the regulation of the homologous somatic recombination events that remove wild-type tumor-suppressor alleles. The discovery reported here that chromosomal polymorphisms can modify tumor multiplicity expands the set of genetic polymorphisms that can modify cancer risk in populations. It is important now to investigate whether this class of polymorphic risk is significant in the human population. The early adenoma of the Min mouse has also permitted us to show that the canonical microsatellite and karyotypic instabilities can be completely supplanted by homologous somatic recombination. It is important to continue to use genetically optimal mouse models to study in depth the other mechanisms known or proposed to mediate the loss of gatekeeper functions in cancer.

Methods

Mouse husbandry and genotyping. Mice were bred and housed at the McArdle Laboratory for Cancer Research under conditions of husbandry approved by the American Association of Laboratory Animal Care. They were maintained on a Purina 5020 diet with 9% fat and 20% protein.

Apc^{Min/+} mice were genotyped as described⁴⁰. We obtained *Rb9* mice on the C57BL/6J genetic background from the Jackson Laboratory Cryopreservation Facility. We identified *Rb9* carriers by karyotyping peripheral blood lymphocytes using a previously published protocol⁴¹. Female *Rb9/+* mice transmitted the translocation chromosome to only 20% of their progeny ($\chi^2 = 22.6$, $P < 0.0005$), whereas males transmitted *Rb9* to only 40% of their progeny ($\chi^2 = 4.26$, $P = 0.039$).

Analysis of intestinal tumors. For each *Apc*^{Min/+} mouse, we removed the entire intestinal tract, flushed it with 1× phosphate buffered saline and laid it out on bibulous paper. We measured tumor sizes with a calibrated eyepiece reticle on a Nikon SMZ-U dissecting microscope at ×10 magnification. We assessed the regional distribution of tumors in the small intestine by counting tumors in each 2-cm section of the small intestine, beginning at the duodenum and ending at the ileocecal junction. We carried out quantitative PCR to assess the allelic status at the *Apc* locus as described⁴.

Interphase FISH. We carried our interphase FISH on mouse and human tissues as described⁴². The *18tel* probe was a biotin-labeled, chromosome-specific cosmid probe obtained from Applied Genetics Laboratories. We isolated BAC probes for specific chromosomal loci from the RPCI-23 B6 BAC library (P. DeJong, Oakland, California, USA) with a PCR product amplified from B6 genomic DNA. The coordinates of the clones are: *Apc*, plate 164, well L14; *18cen*, plate 112, well b21; *14cen*, plate 106, well j24. The *18cen* BAC was isolated with a PCR product from the *Tpl2* gene and lay 2 Mb from the physical end of chromosome 18 (data from <http://mouse.ensembl.org>). The *14cen* probe was 10 Mb from the centromeric end of chromosome 14. We used BAC DNA for FISH after labeling it with digoxigenin by nick translation (Roche). We detected the probes with antibody against digoxigenin labeled with fluorescein isothiocyanate (FITC) or with FITC-avidin. Signals were amplified with rabbit antibody against FITC labeled with AlexaFluor-488 and goat antibody against rabbit labeled with AlexaFluor-488 (Molecular Probes). We counterstained nuclei with propidium iodide.

Analysis of interphase FISH tissues. We used histological sections (5 μm) of normal intestinal epithelium. For each sample (karyotypically normal (+/+), *Rb9/+*, *Rb9/Rb9*), we found cells in which both hybridization signals were present on the same focal plane. We obtained digital images from those cells with a Spot II digital camera (Diagnostic Instruments) mounted on a Zeiss Axiophot microscope. We measured the distance between the two hybridization signals using the ruler tool in Adobe Photoshop 5.5.

Combined FISH and immunohistochemistry. We combined immunohistochemistry with FISH using a previously published protocol⁴³. We used mouse embryonic fibroblasts for karyotypically normal (+/+) and adult primary fibroblasts derived from the body wall for *Rb9/+* and *Rb9/Rb9*. All cells were cultured in Dulbecco's modified Eagle medium supplemented with 10% fetal bovine serum. FISH probes were the same as those used on tissue sections and were detected with antibody against digoxigenin labeled with FITC. The nucleolus was detected with a polyclonal goat antibody against fibrillar (Santa Cruz Biotechnology) and secondary donkey antibody against goat labeled with AlexaFluor-594 (Molecular Probes). We counterstained nuclei with DAPI.

Note: Supplementary information is available on the Nature Genetics website.

Acknowledgments

We dedicate this work to the memory of G. Pontecorvo, who insisted long ago on the importance of somatic recombination for mammalian genetics. The authors thank M. Haigis, L. Clipson, N. Drinkwater, A. Shedlovsky, R. Halberg and I. Riegel for critical reading of the manuscript; M. Newton for the statistical analysis in Web Note A; D. Threadgill for insightful discourse; C. Alexander for the gift of mouse embryonic fibroblasts; and J. Weeks and H. Edwards for histological preparations. This work was supported by grants from the US National Cancer Institute, K.M.H. was supported by a predoctoral training grant from the US National Institutes of Health. This is publication No. 3607 from the Laboratory of Genetics.

Competing interests statement

The authors declare that they have no competing financial interests.

Received 4 September; accepted 24 October 2002.

1. Fearnhead, N.S., Britton, M.P. & Bodmer, W.F. The ABC of APC. *Hum. Mol. Genet.* **10**, 721–733 (2001).
2. Tucker, M., Goldstein, A., Dean, M. & Knudson, A. National Cancer Institute Workshop: the phakomatoses revisited. *J. Natl. Cancer Inst.* **92**, 530–533 (2000).
3. Shoemaker, A.R., Gould, K.A., Luongo, C., Moser, A.R. & Dove, W.F. Studies of neoplasia in the Min mouse. *Biochim. Biophys. Acta* **1332**, F25–F48 (1997).
4. Luongo, C., Moser, A.R., Gledhill, S. & Dove, W.F. Loss of *Apc*⁺ in intestinal adenomas from Min mice. *Cancer Res.* **54**, 5947–5952 (1994).
5. Shoemaker, A.R. et al. A resistant genetic background leading to incomplete penetrance of intestinal neoplasia and reduced loss of heterozygosity in *Apc*^{Min/+} mice. *Proc. Natl. Acad. Sci. USA* **95**, 10826–10831 (1998).
6. Haigis, K.M., Caya, J.G., Reichelderfer, M. & Dove, W.F. Intestinal adenomas can develop with a stable karyotype and stable microsatellites. *Proc. Natl. Acad. Sci. USA* **99**, 8927–8931 (2002).
7. Robertson, W.M.R.B. Chromosome studies. I. Taxonomic relationship shown in the chromosomes of *Tetragidae* and *Acrididae*: V-shaped chromosomes and their significance in *Acrididae*, *Locustidae* and *Grillidae*: chromosome variations. *J. Morphol.* **27**, 179–331 (1916).
8. Gropp, A. et al. Robertsonian karyotype variation in wild house mice from Rhaeto-Lombardia. *Cytogenet. Cell Genet.* **34**, 67–77 (1982).
9. Lane, P.W. & Eicher, E.M. Location of plucked (*pk*) on chromosome 18 of the mouse. *J. Hered.* **76**, 476–477 (1985).
10. Eppig, J.T. & Eicher, E.M. Analysis of recombination in the centromere region of mouse chromosome 7 using ovarian teratoma and backcross methods. *J. Hered.* **79**, 425–429 (1988).
11. Wallace, B.M.N., Searle, J.B. & Everett, C.A. Male meiosis and gametogenesis in wild house mice (*Mus musculus domesticus*) from a chromosomal hybrid zone; a comparison between “simple” Robertsonian heterozygotes and homozygotes. *Cytogenet. Cell Genet.* **61**, 211–220 (1992).
12. Davisson, M.T. & Akeson, E.C. Recombination suppression by heterozygous Robertsonian chromosomes in the mouse. *Genetics* **133**, 649–667 (1993).
13. Dunnett, C.W. Pairwise multiple comparisons in homogeneous variance, unequal sample size case. *J. Am. Stat. Assn.* **75**, 789–795 (1980).
14. Falconer, D.S. & Mackay, T.F.C. *Introduction to Quantitative Genetics* (Longman, Harlow, Essex, 1996).
15. Shoemaker, A.R. et al. *Mlh1* deficiency enhances several phenotypes of *Apc*^{Min/+} mice. *Oncogene* **19**, 2774–2779 (2000).
16. Gould, K.A., Dietrich, W.F., Borenstein, N., Lander, E.S. & Dove, W.F. *Mom1* is a semi-dominant modifier of intestinal adenoma size and multiplicity in *Min*⁺ mice. *Genetics* **144**, 1769–1776 (1996).
17. Cormier, R.T. & Dove, W.F. *Dnmt1*^{N/+} reduces the net growth rate and multiplicity of intestinal adenomas in C57BL/6-multiple intestinal neoplasia (*Min*)⁺ mice independently of *p53* but demonstrates strong synergy with the modifier of *Min-1* (AKR) resistance allele. *Cancer Res.* **60**, 3965–3970 (2000).
18. Merritt, A.J., Gould, K.A. & Dove, W.F. Polyclonal structure of intestinal adenomas in *Apc*^{Min/+} mice with concomitant loss of *Apc*⁺ from all tumor lineages. *Proc. Natl. Acad. Sci. USA* **94**, 13927–13931 (1997).
19. Novelli, M.R. et al. Polyclonal origin of colonic adenomas in an XO/XY patient with FAP. *Science* **272**, 1187–1190 (1996).
20. Shao, C., Stambrook, P.J. & Tischfield, J.A. Mitotic recombination is suppressed by chromosomal divergence in hybrids of distantly related mouse strains. *Nat. Genet.* **28**, 169–172 (2001).
21. Rothstein, R., Michel, B. & Gangloff, S. Replication fork pausing and recombination or “gimme a break.” *Genes Dev.* **14**, 1–10 (2000).
22. Kuzminov, A. DNA replication meets genetic exchange: chromosomal damage and its repair by homologous recombination. *Proc. Natl. Acad. Sci. USA* **98**, 8461–8468 (2001).
23. Luo, G. et al. Cancer predisposition caused by elevated mitotic recombination in Bloom mice. *Nat. Genet.* **26**, 424–429 (2000).
24. Morrison, C. et al. Genetic interaction between PARP and DNA-PK in V(D)J recombination and tumorigenesis. *Nat. Genet.* **17**, 479–482 (1997).
25. Shao, C. et al. Chromosome instability contributes to loss of heterozygosity in mice lacking *p53*. *Proc. Natl. Acad. Sci. USA* **97**, 7405–7410 (2000).
26. Johnson, R.D. & Jasin, M. Double-strand-break-induced homologous recombination in mammalian cells. *Biochem. Soc. Trans.* **29**, 196–201 (2001).
27. Turker, M.S. et al. Solid tissues removed from *ATM* homozygous deficient mice do not exhibit a mutator phenotype for second-step autosomal mutations. *Cancer Res.* **59**, 4781–4783 (1999).
28. de Wind, N., Dekker, M., Berns, A., Radman, M. & te Riele, H. Inactivation of the mouse *Msh2* gene results in mismatch repair deficiency, methylation tolerance, hyperrecombination, and predisposition to cancer. *Cell* **82**, 321–330 (1995).
29. Merriam, J.R. & Garcia-Bellido, A. A model for somatic pairing derived from somatic crossing over with third chromosome rearrangements in *Drosophila melanogaster*. *Mol. Gen. Genet.* **115**, 294–301 (1972).
30. Garcia-Bellido, A. & Wandosell, F. The effect of inversions on mitotic recombination in *Drosophila melanogaster*. *Mol. Gen. Genet.* **161**, 317–321 (1978).
31. Silver, L.M. & Artzt, K. Recombination suppression of mouse t-haplotypes due to chromatin mismatching. *Nature* **290**, 68–70 (1981).
32. Lengauer, C., Kinzler, K.W. & Vogelstein, B. Genetic instability in colorectal cancers. *Nature* **386**, 623–627 (1997).
33. Marx, J. Debate surges over the origin of genomic defects in cancer. *Science* **297**, 544–546 (2002).
34. Nielsen, J. & Wohler, M. Chromosome abnormalities found among 34,910 newborn children: results from a 13-year incidence study in Arhus, Denmark. *Hum. Genet.* **87**, 81–83 (1991).
35. Frydman, N. et al. Assisting reproduction of infertile men carrying a Robertsonian translocation. *Hum. Reprod.* **16**, 2274–2277 (2001).
36. Brasch, J.M. & Smith, D.R. Absence of silver bands in human Robertsonian translocation chromosomes. *Cytogenet. Cell Genet.* **24**, 122–125 (1979).
37. Hagstrom, S.A. & Dryja, T.P. Mitotic recombination map of 13cen–13q14 derived from an investigation of loss of heterozygosity in retinoblastoma. *Proc. Natl. Acad. Sci. USA* **96**, 2952–2957 (1999).
38. Harbour, J.W. Molecular basis of low-penetrance retinoblastoma. *Arch. Ophthalmol.* **119**, 1699–1704 (2001).
39. Shaffer, L.G. & Lupski, J.R. Molecular mechanisms for constitutional chromosomal rearrangements in humans. *Annu. Rev. Genet.* **34**, 297–329 (2000).
40. Su, L.K. et al. Multiple intestinal neoplasia caused by a mutation in the murine homolog of the APC gene. *Science* **256**, 668–670 (1992).
41. Davisson, M.T. & Akeson, E.C. An improved method for preparing G-banded chromosomes from mouse peripheral blood. *Cytogenet. Cell Genet.* **45**, 70–74 (1987).
42. Jacoby, R.F. et al. A juvenile polyposis tumor suppressor locus at 10q22 is deleted from non-epithelial cells in the lamina propria. *Gastroenterology* **112**, 1398–1403 (1997).
43. Bridger, J.M., Herrmann, H., Munkel, C. & Lichter, P. Identification of an interchromosomal compartment by polymerization of nuclear-targeted vimentin. *J. Cell Sci.* **111**, 1241–1253 (1998).

